MITSUBISHI ELECTRIC RESEARCH LABORATORIES
http://www.merl.com

Low-thrust GTO-to-GEO trajectory optimization and tracking

Kalabić, Uroš; Weiss, Avishai; Grover, Piyush

TR2018-117 August 24, 2018

Abstract

In this work, we consider the problem of low-thrust GTO-to-GEO osculating trajectory optimization and tracking. We exploit analytical solutions available in the averaged planar problem and use homotopy methods to obtain fuel- and time-optimal osculating trajectories using direct numerical optimal control tool GPOPS-II. We employ an attitude controller for tracking the thrust vector profile obtained from the optimal trajectories, while maintaining desired solar panel alignment. We simulate the operation of our controller numerically using MATLAB and the high-fidelity Systems Tool Kit (STK) software, and show satisfactory tracking performance of the controller.

AAS/AIAA Astrodynamics Specialist Conference

AAS 18-398

LOW-THRUST GTO-TO-GEO TRAJECTORY OPTIMIZATION AND TRACKING

Uroš Kalabić,* Avishai Weiss,† and Piyush Grover†

In this work, we consider the problem of low-thrust GTO-to-GEO osculating trajectory optimization and tracking. We exploit analytical solutions available in the averaged minimum-energy planar optimal control problem, and use homotopy methods to obtain fuel- and time-optimal osculating trajectories using direct numerical optimal control tool GPOPS-II. We employ an attitude controller for tracking the thrust vector profile obtained from the optimal trajectories, while maintaining desired solar panel alignment. We simulate the operation of our controller numerically using MATLAB and the high-fidelity Systems Tool Kit (STK) software, and show satisfactory tracking performance of the controller.

INTRODUCTION

Electrical propulsion is more efficient than chemical propulsion but produces smaller amounts of thrust. Using chemical thrusters, orbital maneuvers are typically performed using impulses fired at specific times. Because chemical thrusters produce a large amount of thrust, they can cause a large enough change in the orbital parameters to send a satellite into an orbital-transfer trajectory. To achieve the same effect, electrical thrusters must be fired for longer periods of time, perhaps even continuously. In this work, we study the raising of a satellite from geostationary transfer orbit (GTO) to geostationary Earth orbit (GEO) using electrical thrusters.

Our solution to the orbit-raising problem for low-thrust satellites is divided into two components. The first component computes an optimal trajectory prior to flight for both minimum-fuel and minimum-time transfers. The second component is an on-board controller designed to track the optimal trajectory; it consists of an attitude controller that tracks the thrust vector obtained via trajectory optimization, while ensuring that the spacecraft solar panels are always aligned perpendicularly to the Sun.

Our trajectory optimization scheme is based on direct transcription, which is one of the two main numerical approaches for solving optimal control problems, the other being shooting methods. Various analytical techniques have been proposed in the literature to simplify the numerical solution of low-thrust trajectory optimization problems. Among these, orbital averaging methods that exploit the slow-variation in orbital parameters to simplify the problem are popular. Averaging was used along with direct transcription in Reference 1 to obtain minimum-time GTO-to-GEO trajectories, and in Reference 2 to obtain coplanar transfers. The authors of Reference 3 used a parameterized control law and averaging to solve for minimum-time Earth-orbit transfers. Shooting methods

*Research Scientist, Control and Dynamical Systems, Mitsubishi Electric Research Laboratories, 201 Broadway, 8th Floor, Cambridge, MA 02139.

†Principal Research Scientist, Control and Dynamical Systems, Mitsubishi Electric Research Laboratories, 201 Broadway, 8th Floor, Cambridge, MA 02139.

have been used along with a homotopy approach to solve for minimum-fuel Earth-orbit transfers in Reference 4. A sequential quadratic programming approach to direct transcription has also been used to solve for minimum-fuel Earth-orbit transfer with very low thrust.[5] Using averaging, the authors of References 6 and 7 obtained analytical solutions to the averaged coplanar transfers in the minimum-energy case. Reference 8 proposed a novel way of generating a good initial guess and used GPOPS-II[9] to solve the minimum-time GTO-to-GEO problem using direct transcription.

Our scheme is reliant on obtaining a good initial guess, which we do by solving a sequence of optimization problems with sequentially higher fidelity. In the case of minimizing fuel-consumption, at first we obtain an initial guess from the analytical solution to the time-averaged, coplanar-transfer, minimum-energy problem.[6,7] We use this to obtain the solution to the coplanar-transfer, minimum-energy problem. We then find the solution to the case of the non-coplanar transfer. Finally, knowing that there exists a homotopy between the minimum-energy and minimum-fuel trajectories, we find the solutions to a blend of minimum-energy and minimum-fuel costs, gradually changing the cost from minimum-energy to minimum-fuel. In the case of minimizing flight-time, we follow the procedure of Reference 8, where the initial guess for the full optimal control problem is obtained by concatenating solutions of a sequence of modified optimal control problems, each at most one orbit long. The solution of the full problem is then improved via a gradient descent method to escape possible local minima. For both minimum-time as well as minimum-fuel case, GPOPS-II is used to solve the intermediate and final optimal control problems.

Trajectory tracking is achieved by a feedback attitude controller, based on the one provided in Reference 10, which uses reaction wheels on the spacecraft to track a desired attitude profile. The desired attitude profile is uniquely determined from the thrust vector profile, obtained via optimization and the vector pointing in the direction of the Sun. Trajectory tracking is not done directly, *i.e.*, it is open loop. However, by implementing good tracking of the attitude, we are able to track the required thrust closely enough to ensure that the tracking of the trajectory is within specifications and prescribed constraints. Since the trajectory is computed using a high-fidelity dynamic model, which takes into account the major disturbances affecting the spacecraft, namely the J2 and J4 oblateness effects and the Sun's gravitation, open-loop tracking of the trajectory can result satisfactory performance.

A numerical simulation is presented, which uses MATLAB for propagation of attitude dynamics and Systems Tool Kit (STK) for propagation of orbital dynamics. The results show good tracking of the desired trajectory, with errors within the prescribed constraints.

The paper is organized as follows. The next section describes the optimization or the orbit-raising trajectory scheme. The next section describes the attitude-tracking control scheme. The next section provides simulation results obtained using STK. The final section is the conclusion.

TRANSFER FROM GTO TO GEO USING LOW-THRUST PROPULSION

In this work, we design and test a method of transferring a spacecraft from GTO to GEO using low-thrust propulsion. Because of the small amount of force generated by the spacecraft thrusters, our design is based on the assumption that thrusters will fire continuously at maximum output for the duration of the mission. We consider two types of trajectories: one minimizing fuel expended and the other minimizing total mission time. The trajectories are precomputed using a high-fidelity optimization model taking into account the major forces acting on the satellite in space. In flight, the spacecraft tracks these trajectories using a control system that fires the thruster in the direction

element	value
GTO semi-major axis (km)	24,522
GTO eccentricity	0.72
GTO inclination (°)	28.5
GEO semi-major axis (km)	42,164
GEO eccentricity	0
GEO inclination (°)	0

Table 1: Specifications of initial GTO orbit and final GEO orbit

that is tangential to the trajectory, using a feedback controller to track the desired attitude using a 3-axis reaction wheel assembly.

According to the mission specifications, our design must achieve certain requirements. The initial GTO and final GEO orbits have the specifications given in Table 1. The specifications for the tracking component of the mission design are as follows. Firstly, the total amount of thrust available is no more than $T = 0.895$N. Secondly, the angular velocities of the reaction wheels must stay within 4000rpm. Secondly, to allow for enough solar-power generation, the spacecraft's solar panels can point no more than 15° away from the Sun. Finally, to allow for insertion into GEO, the tracking error at the end of the mission must be no more than,

$$|\Delta a(t_f)| \leq 10\text{km}, \tag{1a}$$
$$|\Delta e(t_f)| \leq 10^{-3}, \tag{1b}$$
$$|\Delta i(t_f)| \leq 0.1^\circ, \tag{1c}$$
$$|\Delta L(t_f)| \leq 0.1^\circ, \tag{1d}$$

where a is the semi-major axis of the spacecraft orbit, e is the eccentricity, i is the inclination, L is the longitude, and t_f is the time at the end of the mission. The symbol Δ is used to denote deviation from the nominal value.

The desired trajectory, along with the requirements on the thruster and solar-paned axes, uniquely describes an attitude that must be tracked by the controller. The attitude controller is a feedback controller, but it does not make corrections being made for deviations from the nominal trajectory. As such, the tracking of the precomputed trajectories is done in an open-loop fashion and there is no *a priori* guarantee that the requirements listed above will be achieved. For this reason, in order to rigorously validate our design, we found it necessary to simulate the mission in the high fidelity simulator STK.

In the rest of this section, we describe the designs of our trajectory optimization scheme and attitude control system in detail.

Orbit-Raising Design

We consider a design comprised of two parts. The first part is the determination of the trajectory optimization, which is computed numerically prior to launch of the spacecraft. The output of the optimization scheme is a trajectory and the required thrust profile. The second part of the design consists of an attitude tracking controller that is designed to closely track the desired thrust vector and align the spacecraft solar panels with the Sun. After launch, the controller achieves the desired

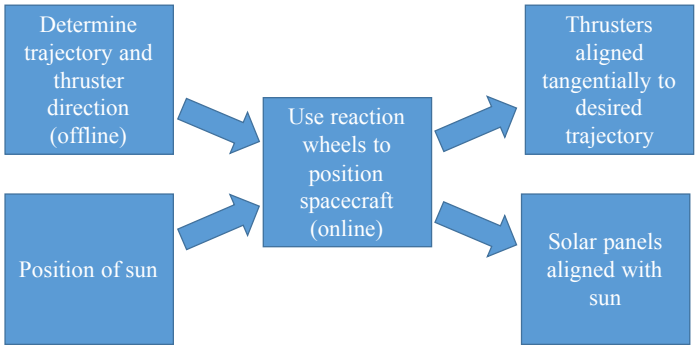

Figure 1: Schematic of the orbit-raising design

trajectory by ensuring that the thrusters always point in the prescribed direction. We provide a schematic of the design in Figure 1 and, in the following, we discuss the two components of our design.

Optimal Trajectory Design Via Solution of Low-Thrust Optimal Control Problem

We solve the low-thrust optimal control problem using a direct transcription method[11] and the pseudo-spectral numerical optimal control tool GPOPS-II.[9]

The dynamical equation governing the spacecraft motion is given by,

$$\ddot{\mathbf{x}} = -\mu \frac{\mathbf{x}}{\|\mathbf{x}\|^3} + \mathbf{a}, \tag{2}$$

where $\mathbf{x}$ is the position of the satellite in an inertial frame centered at the Earth, $\mathbf{a}$ is the acceleration due to thrusting acting on the satellite measured in the same frame and μ is the gravitational parameter of the Earth. An alternative to these equations of motion is to use the modified equinoctial coordinates,[11] which avoid singularities and result in a more robust optimization scheme. In these coordinates, the acceleration $\mathbf{u} = \begin{bmatrix} u_r & u_\theta & u_h \end{bmatrix}^{\mathrm{T}}$ is expressed in the radial-orthoradial frame and satisfies $\mathbf{a} = u_r \hat{r} + u_\theta \hat{\theta} + u_h \hat{h}$, where $\hat{r} = \mathbf{x}/\|\mathbf{x}\|$, $\hat{\theta} = \dot{\mathbf{x}}/\|\dot{\mathbf{x}}\|$, $\hat{h} = \hat{r} \times \hat{\theta}$. The equations of motion are given by,

$$\dot{\mathbf{y}} = \sum_{i=r,\theta,h} \mathbf{f}_i(L, \mathbf{y}) u_i, \tag{3a}$$

$$\dot{L} = g_0(\mathbf{y}) + g_h(L, \mathbf{y}) u_h, \tag{3b}$$

where the elements of $\mathbf{y} = \begin{bmatrix} p & e_x & e_y & h_x & h_y \end{bmatrix}^{\mathrm{T}}$, along with L, are the modified equinoctial coordinates; p is the semi-latus rectum, the pair (e_x, e_y) comprises the eccentricity vector, the pair (h_x, h_y) comprises the angular momentum vector, and L is the longitudinal position along the tra-

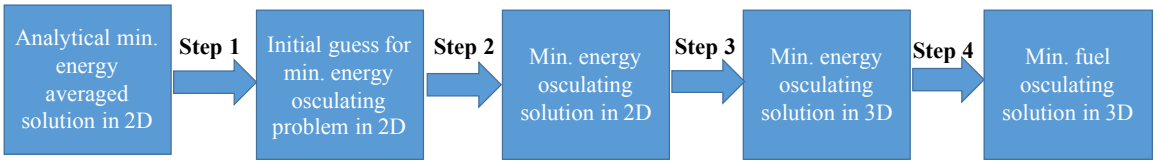

Figure 2: Illustration of the multi-step optimization scheme to obtain a 3D osculating minimum-fuel trajectory

jectory in radians. The expressions for $\mathbf{f}_i$ and g_0 and g_h are given by,

$$\mathbf{f}_r = \begin{bmatrix} 0 \\ \sqrt{\frac{p}{\mu}}\sin L \\ -\sqrt{\frac{p}{\mu}}\cos L \\ 0 \\ 0 \end{bmatrix}, \; \mathbf{f}_\theta = \begin{bmatrix} \frac{2p}{q}\sqrt{\frac{p}{\mu}} \\ \sqrt{\frac{p}{\mu}}\frac{1}{q}\left((q+1)\cos L + e_x\right) \\ \sqrt{\frac{p}{\mu}}\frac{1}{q}\left((q+1)\sin L + e_y\right) \\ 0 \\ 0 \end{bmatrix}, \; \mathbf{f}_h = \begin{bmatrix} 0 \\ -\sqrt{\frac{p}{\mu}}\frac{e_y}{q}(h_x \sin L - h_y \cos L) \\ \sqrt{\frac{p}{\mu}}\frac{e_x}{q}(h_x \sin L - h_y \cos L) \\ \sqrt{\frac{p}{\mu}}\frac{s^2 \cos L}{2q} \\ \sqrt{\frac{p}{\mu}}\frac{s^2 \sin L}{2q} \end{bmatrix},$$

$$g_0 = \sqrt{\mu p}\left(\frac{q}{p}\right)^2, \; g_h = \sqrt{\frac{p}{\mu}}(h_x \sin L - h_y \cos L),$$

where $q = 1 + e_x \cos L + e_y \sin L$, $r = p/q$, $\alpha^2 = h_x^2 - h_y^2$, and $s^2 = 1 + \sqrt{h_x^2 + h_y^2}$. The reason for separating L from the rest of the elements of $\mathbf{y}$ is that it is treated as an independent variable in the computation of the optimal control. By doing this, we simplify the computation[8] and are still able to relate L to the actual time t by using Eq. (3b).

The acceleration vector $\mathbf{u}$ can be decomposed into a control component $\mathbf{u}_T$ and a disturbance component $\mathbf{u}_d$,

$$\mathbf{u} = \mathbf{u}_T + \mathbf{u}_d. \tag{4}$$

The disturbance acceleration $\mathbf{u}_d$ consists of all accelerations acting on the satellite not due to thrust. The main disturbances expected to be encountered during the mission, *i.e.*, the disturbances due to the J2 and J4 oblateness effects and the gravitational pulls of the Sun and Moon, are accounted for during the optimization process using analytical expressions or ephemeris data.

Minimum-fuel problem. The main challenge in computing (near) optimal solutions using direct transcription is obtaining a high-quality initial guess; since low-thrust trajectories consist of hundreds of orbits with many local minima, a good initial guess is of critical importance. To address this challenge, we adopt a multi-step approach that uses analytical solutions available in the averaged 2D minimum energy problem, and exploit its relation to the minimum fuel problem. The approach is summarized in the schematic of Figure 2.

We begin by replicating the analysis of Reference 7, where the authors obtain an analytical expression for the minimum-energy trajectory by using an averaging method. We first note that the dynamics (3) can be written with L as the independent variable,

$$\frac{d\mathbf{y}}{dL} = \frac{1}{g_0(\mathbf{y}) + g_h(L,\mathbf{y})v_h} \sum_{i=r,\theta,h} \mathbf{f}_i(L,\mathbf{y})u_i. \tag{5}$$

Consider the problem of minimizing the thruster energy over the time span $[0, t_f]$ with normalized thrust $\mathbf{v} = \begin{bmatrix} v_r & v_\theta & v_h \end{bmatrix}^{\mathrm{T}} = \mathbf{u}/\varepsilon$,

$$\int_0^{t_f} \varepsilon^2 \|\mathbf{v}\|^2 dt. \tag{6}$$

With a change of independent variable, the cost function becomes,

$$\int_0^{L_f} \frac{\varepsilon^2 \|\mathbf{v}\|^2}{g_0(\mathbf{y}) + \varepsilon g_h(L, \mathbf{y}) v_h} dL, \tag{7}$$

where $L_f = L(t_f)$. Assuming a solution exists, the Hamiltonian of the above problem can be expressed as,

$$\begin{aligned} H_\varepsilon(L, \mathbf{y}, \boldsymbol{\lambda}, \mathbf{v}) &= \frac{\varepsilon^2}{g_0 + \varepsilon g_h v_h} \left(-\frac{1}{2}\|\mathbf{v}\|^2 + \sum_{i=r,\theta,h} \boldsymbol{\lambda}^{\mathrm{T}} \mathbf{f}_i \right), \\ &= \frac{\varepsilon^2}{g_0} \left(1 - \varepsilon \frac{g_h}{g_0} + \cdots \right) \left(-\frac{1}{2}\|\mathbf{v}\|^2 + \sum_{i=r,\theta,h} \boldsymbol{\lambda}^{\mathrm{T}} \mathbf{f}_i \right), \\ &= \frac{\varepsilon^2}{g_0} \left(-\frac{1}{2}\|\mathbf{v}\|^2 + \sum_{i=r,\theta,h} \boldsymbol{\lambda}^{\mathrm{T}} \mathbf{f}_i \right) + o(\varepsilon^2), \end{aligned}$$

where $\boldsymbol{\lambda}$ is the costate vector. Neglecting higher-order terms, taking the maximum, and setting $\varepsilon = 1$ for convenience, the true Hamiltonian becomes,

$$H(L, \mathbf{y}, \boldsymbol{\lambda}) = \frac{1}{2g_0} \sum_{i=r,\theta,h} (\boldsymbol{\lambda}^{\mathrm{T}} \mathbf{f}_i)^2. \tag{8}$$

Since the true Hamiltonian is periodic in L with period 2π, we can take define the averaged Hamiltonian as,

$$\bar{H}(\mathbf{y}, \boldsymbol{\lambda}) = \frac{1}{2\pi} \int_0^{2\pi} H(L, \mathbf{y}, \boldsymbol{\lambda}) dL. \tag{9}$$

As shown in Reference 7, the averaged Hamiltonian system is integrable. In particular, the authors provide an analytical expression for the minimum energy trajectories in the case of a coplanar orbital transfer, which we use as the starting point for our optimization procedure. The averaged trajectory is a geodesic for the corresponding sub-Riemannian problem and describes the curve of the optimal trajectory in the (p, e)-plane. In that analysis, it was further established that the product of transfer time and maximum thrust is a constant for the case of very low thrust, meaning that time is inversely proportional to amount of thrust.

The computation of the optimal trajectory follows the steps introduced in Figure 2. They are described in the following.

1. We begin by estimating N, the number of revolutions for a given thrust magnitude. We divide the analytically available 2D optimal trajectory, *i.e.*, geodesic, into N equally spaced segments in L, and label the points $(p_i, e_i)_{i=1}^N$. Each segment represents one orbit or revolution of the osculating trajectory. A sequence of optimal control problems are solved to obtain

a guess for the osculating elements and the control profile for each orbit. Each of these optimal control problems has its initial condition on the geodesic curve, and aims to minimize the distance between the endpoint of the current segment and the next point on the geodesic curve. An initial guess for each segment is obtained by continuously thrusting in the tangential direction at full thrust. Hence, the optimal control problem for the i-th segment is solved over the L-interval $[i2\pi, (i+1)2\pi]$ to minimize the cost function subject to the dynamics (3a),

$$J_i = \frac{(p(L_{f,i}) - p_{i+1})^2}{(1+p_{i+1})^2} + \frac{e_x(L_{f,i})^2 + e_y(L_{f,i})^2 - e_{i+1}^2}{(1+e_{i+1}^2)^2}, \tag{10}$$

where $L_{f,i} = (i+1)2\pi$. The optimization is subject to the thrust constraint $\|u(L)\| \leq T$, and has initial condition $p = a_i, e_x = e_i, e_y = 0, h_x = \tan(i_{GTO}/2), h_y = 0$, with the value for initial inclination i_{GTO} being set to 28.5° as according to Table 1.

2. An initial guess for the full, osculating 2D trajectory is obtained by patching together the individual segments obtained in Step 1. This initial guess is used to solve the 2D optimal control problem with energy as the cost function to be minimized.

3. The solution of Step 2 is modified to include an inclination that decreases linearly in L and achieves 0 at the final time. This modified trajectory is used as an initial guess for solving the 3D minimum-energy optimal control problem.

4. In the final step, a homotopy[12] is carried out by iteratively solving the optimal control problems with the following cost function while gradually decreasing the homotopy parameter α from 1 to 0,

$$J = \int_0^T |u(t)|(\alpha|u(t)| + (1-\alpha))dt. \tag{11}$$

At each iteration, the solution from the previous iteration is used as an initial guess, with the solution for the case where $\alpha = 1$ having been obtained in Step 3.

Minimum-time problem. Unlike the minimum-fuel case, the optimal trajectory for minimum-time case cannot be obtained via a homotopy from an analytically derived solution. It is known that the time-optimal trajectory requires the thruster to fire continuously at maximum thrust. It is therefore necessary to determine the profile of the direction of the thrust vector that minimizes the time taken to transfer the satellite from GTO to GEO. For obtaining minimum-time optimal trajectories, we obtain the initial guesses using a two-step process using methods described in Reference 8. Specifically, a sequence of trajectory optimization problems are solved to obtain segments of the full osculating trajectory, where each segment is at most one revolution long. Each of these optimization problems are initialized at the end-point of the previous segment, and minimize the distance between the desired final condition and its own end point, with the distance being measured in (a, e, i) coordinates. An initial guess for each segment is obtained by continuously thrusting in the tangential direction. This process is continued until the final end point is close to a point on GEO. Once an initial guess for the full trajectory is available, the minimum time problem is solved with a constraint on the final cumulative longitude L_f. A gradient descent in L_f is then carried out to escape possible local minima and obtain candidates for globally time-optimal solutions.

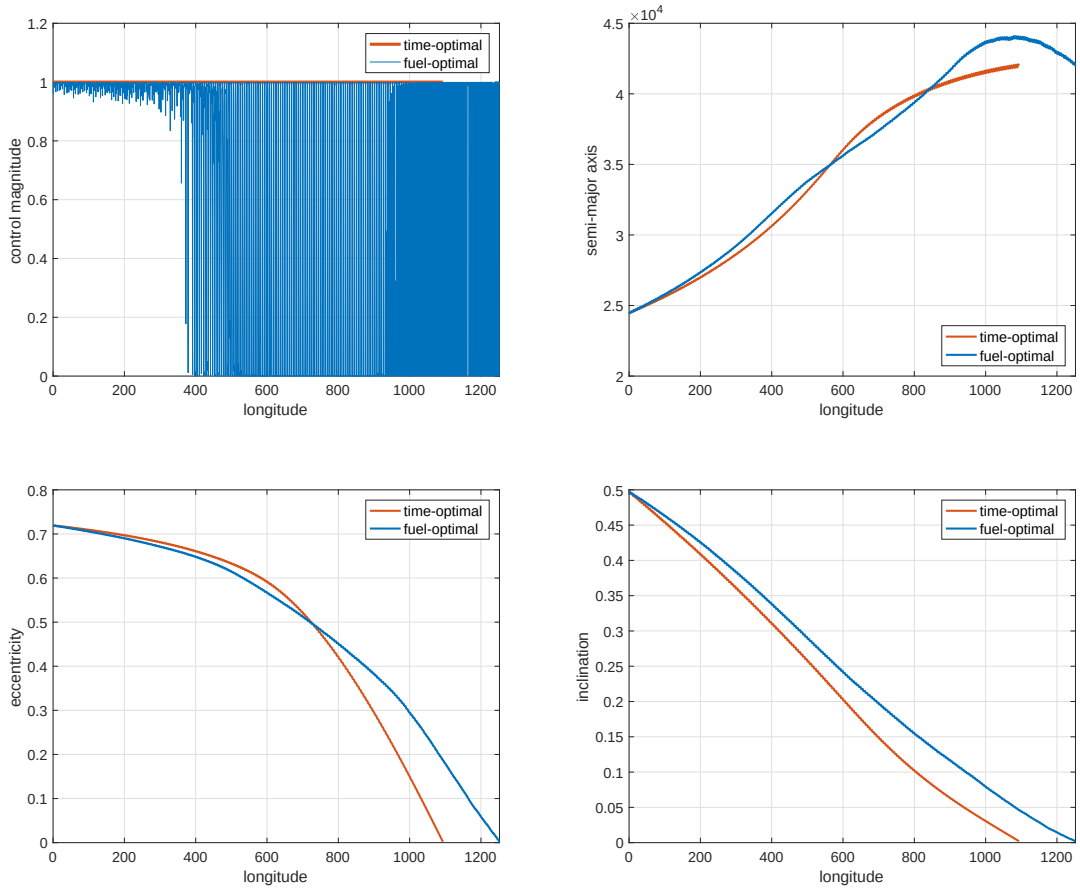

Figure 3: Control magnitude (top-left), semi-major axis (top-right), eccentricity (bottom-left), and inclination (bottom-right) profiles for fuel- and time-optimal trajectories

Computational Results

In Fig. 3, we show the control profile, the semi-major axis, eccentricity and inclination for both fuel-optimal and time-optimal trajectories. For the fuel-optimal case, the maximum mission time is constrained to be 157 days. Note that the numerically computed fuel-optimal trajectory exhibits an almost on-off profile, without it being explicitly enforced during the optimization; theoretically, the optimal profile should be on-off.[6] The duration of time-optimal trajectory is 127.6 days with $\Delta V = 2.65$ km/s. The fuel optimal trajectory is 156.9 days long with $\Delta V = 2.32$ km/s.

The computational cost of computing the minimum-fuel trajectory is dominated by the first step. On a desktop computer with a single Intel Xeon 3.67GHz processor, Step 1 takes an average of about 120 minutes. Steps 2 through 4 take an additional 30 minutes, depending upon the tolerances in the nonlinear programming solver and GPOPS-II.

ATTITUDE TRACKING

Given a time-history of the desired thrust vector $\mathbf{u}_T$, obtained as a solution to the optimal orbit-raising problem, we need to design a control scheme to align the thrust vector of the spacecraft with

$\mathbf{u}_T$ so that we track the orbit raising trajectory. The thrust vector, aligned with the x-axis in the body frame, does not on its own uniquely determine the spacecraft orientation. A unique orientation is obtained when we consider the constraint on the solar panel axis, which requires that we point the spacecraft solar panels toward the Sun at all times. The panels are aligned with the z-axis in the spacecraft body frame and, since they can rotate about this axis, they can therefore align themselves with the Sun as long as the z-axis is close to perpendicular to the Sun axis. We therefore define the desired rotation matrix $\mathbf{R}_d$ as,

$$\mathbf{R}_d = \begin{bmatrix} \mathbf{r}_1 & \mathbf{r}_2 & \mathbf{r}_1^{\times}\mathbf{r}_2 \end{bmatrix}, \tag{12}$$

where $\mathbf{r}_1 = \mathbf{R}_H^{\mathrm{T}}\mathbf{u}_T$ is the thrust vector in the inertial frame, $\mathbf{R}_H$ is the rotation matrix into Hill's frame, $\mathbf{r}_2 = \tilde{\mathbf{s}}/\|\tilde{\mathbf{s}}\|$, and $\tilde{\mathbf{s}} = \mathrm{Proj}_{\mathbf{r}_1}^{\perp}(\mathbf{s})$ is the projection of the vector from the spacecraft to the Sun $\mathbf{s}$ in the inertial frame onto the plane perpendicular to $\mathbf{r}_1$, whenever $\mathbf{s}$ is not parallel to $\mathbf{r}_1$. Practically speaking, considering that numerical precision is very high, these two vectors should never be parallel – if highly improbable case that their directions coincide, we take the previously computed $\tilde{\mathbf{s}}$ as a solution.

To track $\mathbf{R}_d$, we use the control method from Reference 10. To describe the control scheme, we begin by introducing the spacecraft dynamics,

$$\dot{\mathbf{R}} = \dot{\mathbf{R}}\boldsymbol{\omega}^{\times}, \tag{13a}$$

$$\mathbf{J}\dot{\boldsymbol{\omega}} = -\boldsymbol{\omega}^{\times}(\mathbf{J}\boldsymbol{\omega} + \mathbf{J}_{\alpha}\boldsymbol{\nu}) - \mathbf{J}_{\alpha}\mathbf{u}_{\alpha}, \tag{13b}$$

$$\dot{\boldsymbol{\nu}} = \mathbf{u}_{\alpha}, \tag{13c}$$

where $\mathbf{R}$ is the spacecraft rotation matrix, $\mathbf{J}$ is the moment of inertia of the spacecraft in the body frame, and $\boldsymbol{\omega}$ is the angular velocity. The spacecraft is equipped with three reaction wheels which control the orientation. The moment of inertial due to these wheels is given by $\mathbf{J}_{\alpha}$ and their speeds are given by the components of $\boldsymbol{\nu}$. The accelerations of the wheels are the control inputs $\mathbf{u}_{\alpha}$.

The control input is composed of two parts,

$$\mathbf{u}_{\alpha} = \mathbf{J}_{\alpha}^{-1}(\mathbf{v}_1 + \mathbf{v}_2), \tag{14}$$

where,

$$\mathbf{v}_1 = -(\mathbf{J}\boldsymbol{\omega} + \mathbf{J}_{\alpha}\boldsymbol{\nu}) - \mathbf{J}(K_1\dot{\mathbf{S}} + \tilde{\boldsymbol{\omega}}^{\times}\boldsymbol{\omega} - \mathbf{R}^{\mathrm{T}}\dot{\boldsymbol{\omega}}_d),$$
$$\mathbf{v}_2 = -K_v(\tilde{\boldsymbol{\omega}} + K_1\dot{\mathbf{S}}) - K_p\mathbf{S}.$$

The first term in the controller $\mathbf{v}_1$ is designed to ensure close tracking. The term $\mathbf{S}$ is an error term, given by,

$$\mathbf{S} = \sum_{i=1}^{3} a_i(\tilde{\mathbf{R}}^{\mathrm{T}}\mathbf{e}_i)^{\times}\mathbf{e}_i, \tag{15}$$

where $a_i > 0$, $i = 1, 2, 3$ are penalty weights, $\mathbf{e}_i$ is the i-th elementary vector, and where $\tilde{\mathbf{R}} = \mathbf{R}_d^{\mathrm{T}}\mathbf{R}$. The term $\tilde{\boldsymbol{\omega}} = \boldsymbol{\omega} - \boldsymbol{\omega}_d$ is the error in desired angular velocity, computed numerically from $\tilde{\mathbf{R}}$; $\dot{\boldsymbol{\omega}}_d$ is also computed numerically. The second term in the controller $\mathbf{v}_2$ is designed to control the speed of convergence. The term $\dot{\mathbf{S}}$ is given by the analytically derived expression,

$$\dot{\mathbf{S}} = \sum_{i=1}^{3} a_i((\tilde{\mathbf{R}}^{\mathrm{T}}\mathbf{e}_i)^{\times}\tilde{\boldsymbol{\omega}})^{\times}\mathbf{e}_i. \tag{16}$$

The controller is guaranteed to asymptotically stabilize the spacecraft attitude almost-globally. In Reference 10, the authors provide a Lyapunov function proving stability of the spacecraft attitude dynamics under this control.

STK SIMULATION RESULTS

In this section, we present numerical simulation results obtained with MATLAB and STK software. For export control reasons, we were unable to simulate the spacecraft attitude dynamics using STK. Therefore, we used MATLAB to propagate the differential equations describing the attitude dynamics (13) to obtain the spacecraft rotation $\mathbf{R}$. We then passed the first column of this rotation matrix to STK as the thrust vector. The MATLAB simulation results for the attitude tracking are presented in Figures 4-5 and the STK simulation is presented in Figures 6–9.

From the results it is clear that we have achieved the required specifications. Firstly, as can be seen in Figure 4 the rotation wheel stay well below their maximum speed of 4000rpm. In Figure 5, we can see that the constraint on solar panel alignment is also enforced, as the Euler angle errors stay below 3°, which is well below 15°. Furthermore, we have shown satisfactory tracking of the nominal trajectory. In Figures 6–9, we can see that all constraints on the spacecraft final orbit (1) have been achieved.

CONCLUSION

We have presented a scheme for raising the orbit of a spacecraft from GTO to GEO. The scheme consists of two components: The first component is the design of the optimal trajectory and the second component is the in-flight, tracking component. The design of the trajectory was based on a direct transcription method, in which multiple steps were required to obtain improved initial guesses for use in the optimization software GPOPS-II. The trajectories corresponding to both a minimum-fuel and a minimum-time problem were obtained. The tracking component was designed to align the thrust vector of the spacecraft in the desired direction and to align the spacecraft solar panels with the Sun. The controller used to achieve this is a feedback controller on the spacecraft attitude and receives no feedback from trajectory error.

A numerical simulation was performed using STK for propagation of orbital dynamics and MATLAB for propagation of attitude dynamics. The spacecraft tracked the minimum-time trajectory within the prescribed constraints, thereby showing good tracking.

REFERENCES

[1] C. A. Kluever and S. R. Oleson, "Direct approach for computing near-optimal low-thrust earth-orbit transfers," *J. Spacecraft Rockets*, Vol. 35, No. 4, 1998, pp. 509–515.

[2] C. M. Haissig, K. D. Mease, and N. X. Vinh, "Minimum-fuel, power-limited transfers between coplanar elliptical orbits," *Acta Astronaut.*, Vol. 29, No. 1, 1993, pp. 1–15.

[3] G. Yang, "Direct optimization of low-thrust many-revolution earth-orbit transfers," *Chinese J. Aeronaut.*, Vol. 22, No. 4, 2009, pp. 426–433.

[4] T. Haberkorn, P. Martinon, and J. Gergaud, "Low thrust minimum-fuel orbital transfer: a homotopic approach," *J. Guid. Control Dynam.*, Vol. 27, No. 6, 2004, pp. 1046–1060.

[5] J. T. Betts, "Very low-thrust trajectory optimization using a direct SQP method," *J. Comput. Appl. Math.*, Vol. 120, No. 1-2, 2000, pp. 27–40.

[6] S. Geffroy and R. Epenoy, "Optimal low-thrust transfers with constraints–generalization of averaging techniques," *Acta Astronaut.*, Vol. 41, No. 3, 1997, pp. 133–149.

[7] B. Bonnard and J.-B. Caillau, "Riemannian metric of the averaged energy minimization problem in orbital transfer with low thrust," *Ann. I. H. Poincaré–An.*, Vol. 24, 2007, pp. 395–411.

[8] K. F. Graham and A. V. Rao, "Minimum-time trajectory optimization of multiple revolution low-thrust earth-orbit transfers," *J. Spacecraft Rockets*, Vol. 52, No. 3, 2015, pp. 711–727.

[9] M. A. Patterson and A. V. Rao, "GPOPS-II: A MATLAB software for solving multiple-phase optimal control problems using hp-adaptive Gaussian quadrature collocation methods and sparse nonlinear programming," *ACM T. Math. Software*, Vol. 41, No. 1, 2014, pp. 1:1–37.

[10] A. Weiss, I. Kolmanovsky, D. S. Bernstein, and A. Sanyal, "Inertia-free spacecraft attitude control using reaction wheels," *J. Guid. Control Dynam.*, Vol. 36, No. 5, 2013, pp. 1425–1439.

[11] J. T. Betts, *Practical Methods for Optimal Control Using Nonlinear Programming*, ch. 5. Philadelphia: SIAM, 2001.

[12] F. Jiang, H. Baoyin, and J. Li, "Practical techniques for low-thrust trajectory optimization with homotopic approach," *J. Guid. Control Dynam.*, Vol. 35, No. 1, 2012, pp. 245–258.

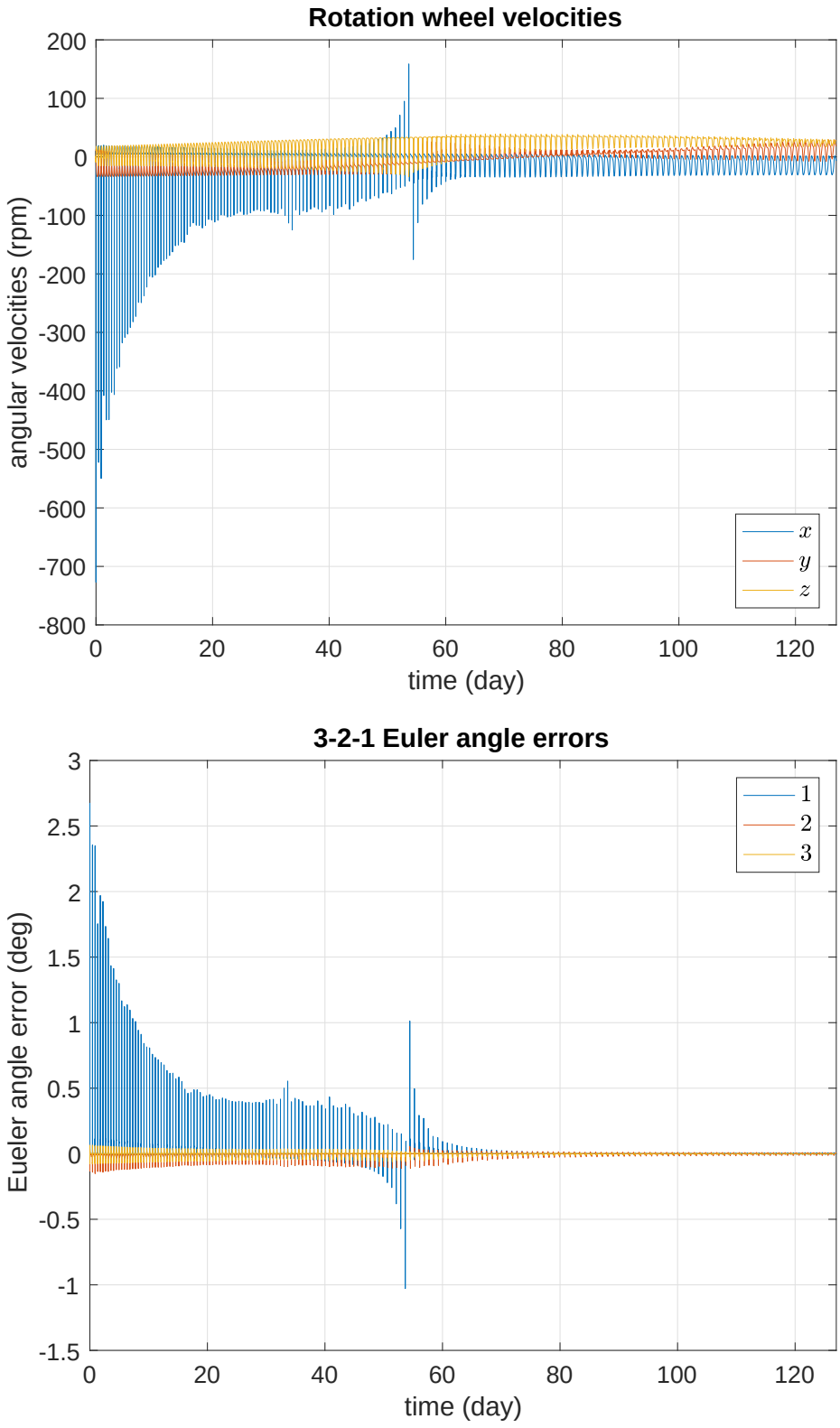

Figure 4: Time-histories of rotation wheels (top) and pointing error measured in 3-2-1 Euler angles (bottom)

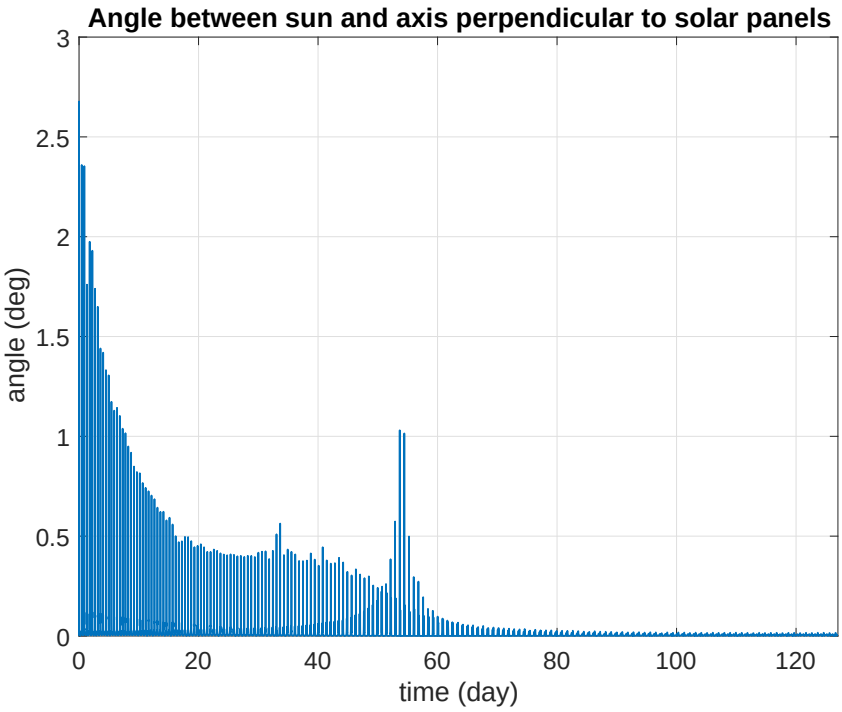

Figure 5: Time-history of angle between Sun and axis perpendicular to solar panels

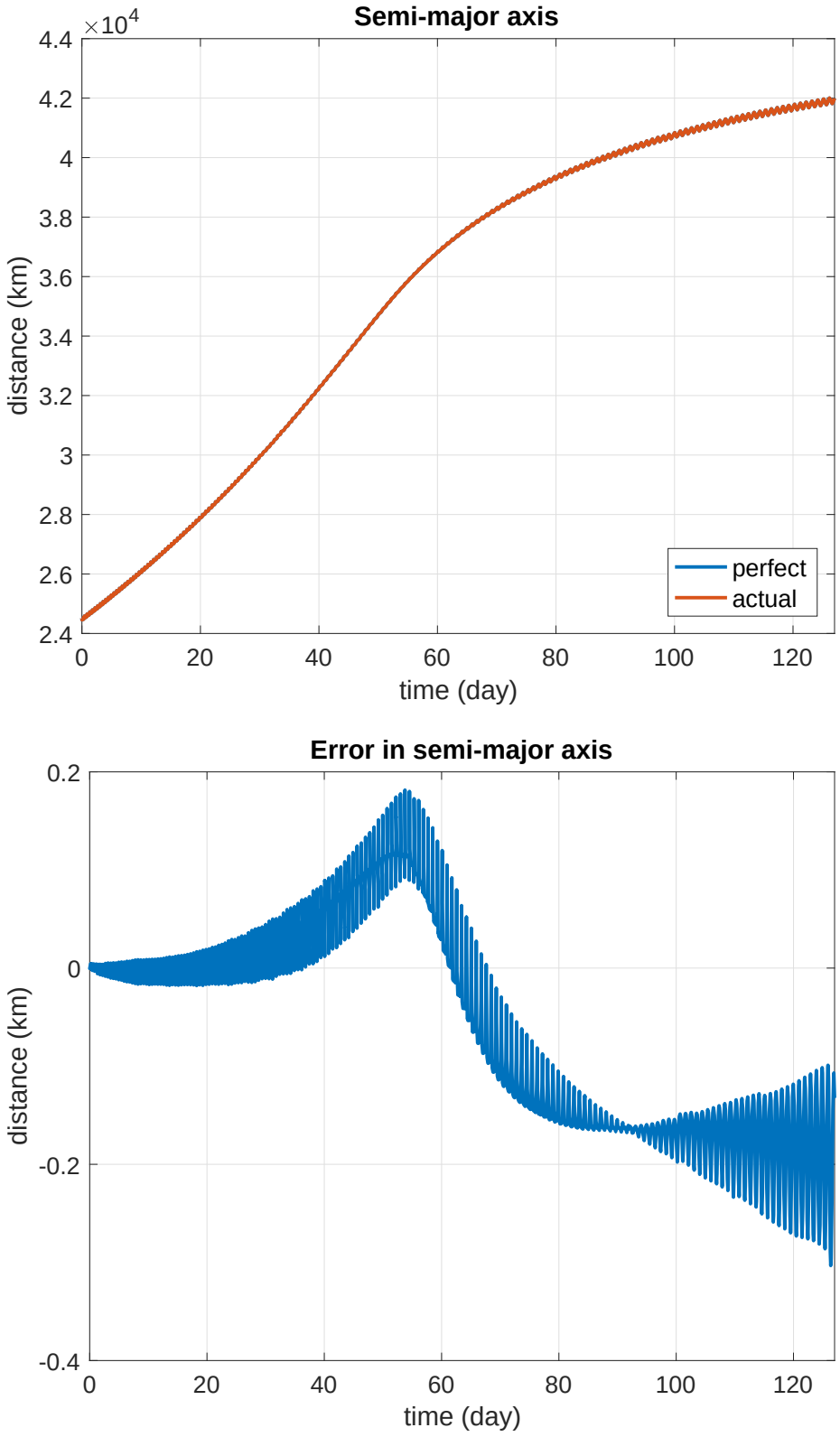

Figure 6: Time-histories of semi-major axis (top) for both perfect (blue) and actual tracking (red) and error in the semi-major axis between perfect tracking and actual tracking (bottom)

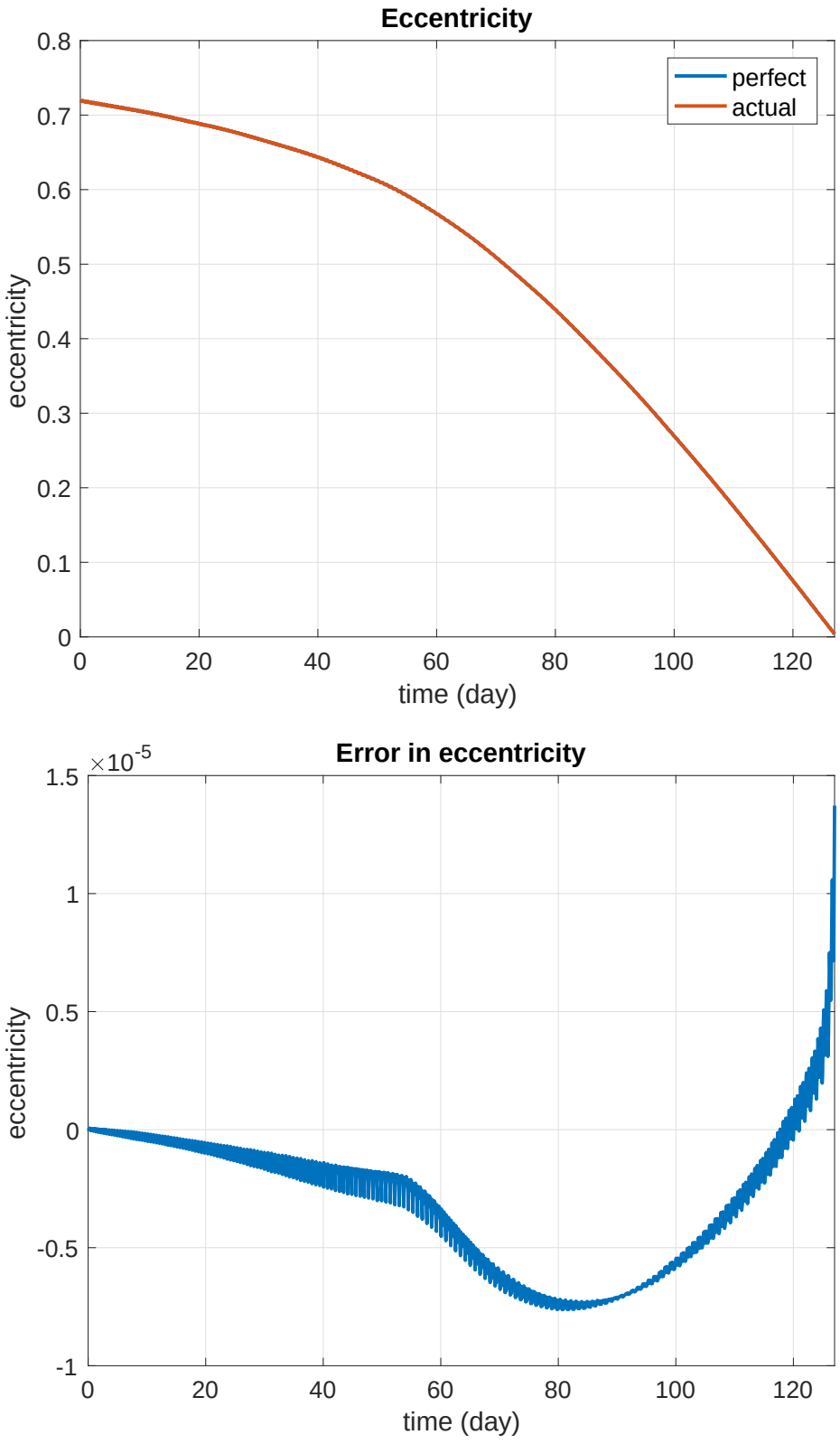

Figure 7: Time-histories of eccentricity (top) for both perfect (blue) and actual tracking (red) and error in the eccentricity between perfect tracking and actual tracking (bottom)

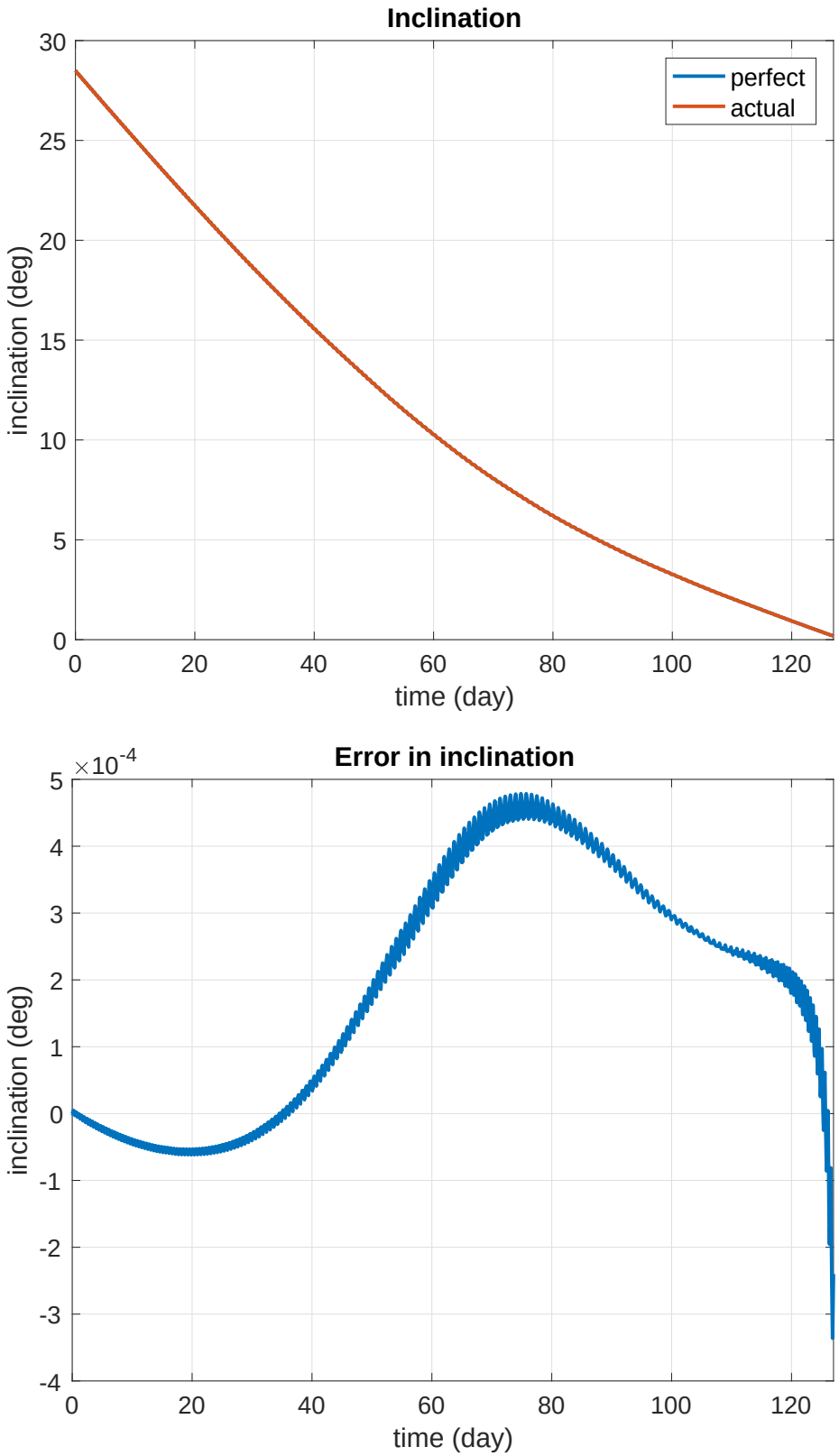

Figure 8: Time-histories of inclination (top) for both perfect (blue) and actual tracking (red) and error in the inclination between perfect tracking and actual tracking (bottom)

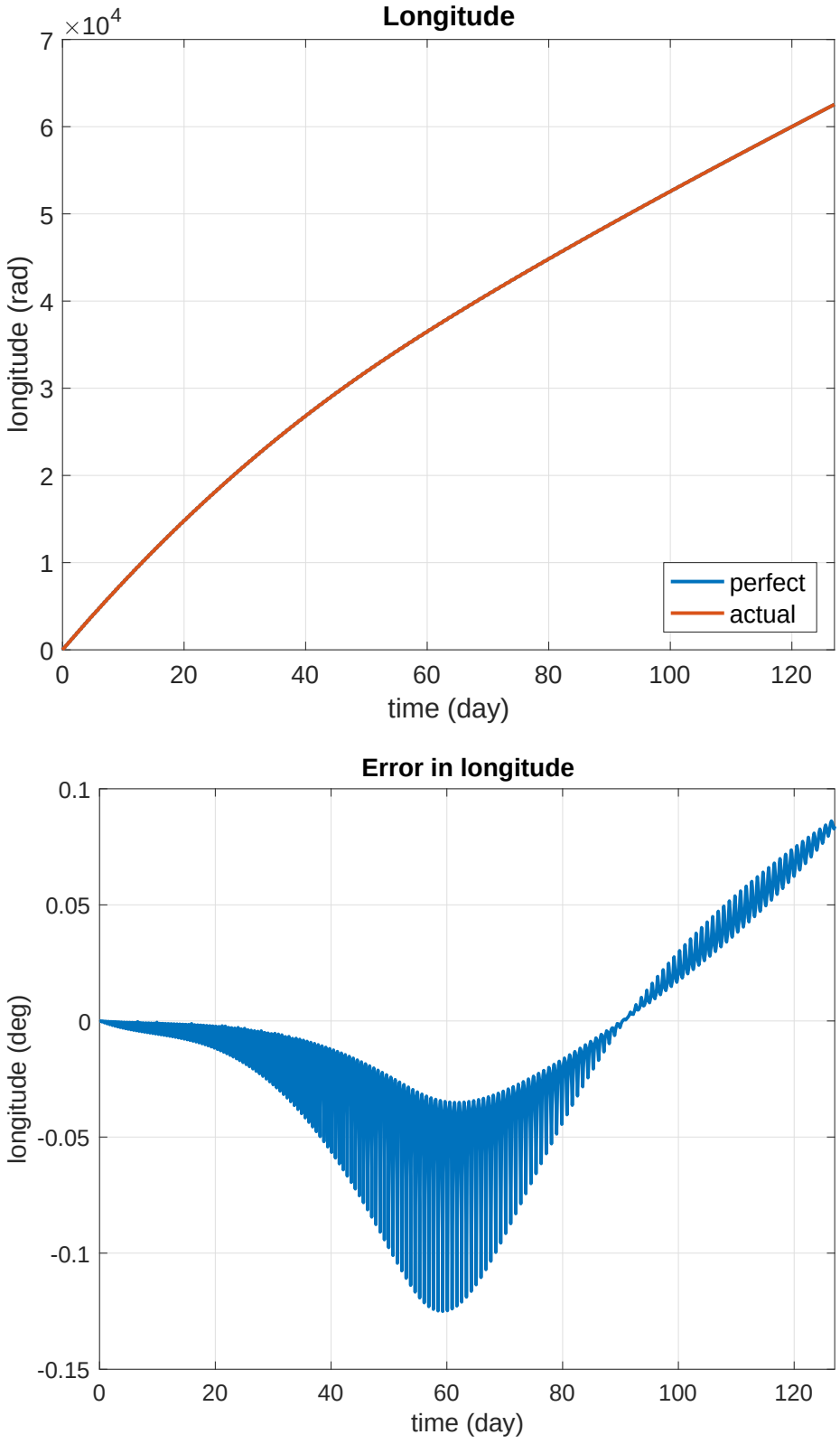

Figure 9: Time-histories of longitude (top) for both perfect (blue) and actual tracking (red) and error in the longitude between perfect tracking and actual tracking (bottom)